*Astronomy & Astrophysics* manuscript no. fams
September 26, 2011


# Constraining the cometary flux through the asteroid belt during the Late Heavy Bombardment

M. Brož[1], A. Morbidelli[2], W.F. Bottke[3], J. Rozehnal[1], D. Vokrouhlický[1], D. Nesvorný[3]

[1] Institute of Astronomy, Charles University, Prague, V Holešovičkách 2, 18000 Prague 8, Czech Republic, e-mail: mira@sirrah.troja.mff.cuni.cz, rozehnal@observatory.cz, davok@cesnet.cz
[2] Observatoire de la Côte d'Azur, BP 4229, 06304 Nice Cedex 4, France, e-mail: morby@oca.eu
[3] Department of Space Studies, Southwest Research Institute, 1050 Walnut St., Suite 300, Boulder, CO 80302, USA, e-mail: bottke@boulder.swri.edu, davidn@boulder.swri.edu

Received ???; accepted ???

**ABSTRACT**

*Context.* In the Nice model, the Late Heavy Bombardment (LHB) is related to an orbital instability of giant planets which causes a fast dynamical decay of a transneptunian cometary disk (Gomes et al. 2005).
*Aims.* We study effects produced by these hypothetical cometary projectiles on main-belt asteroids. According to a "standard" model for the size-frequency distribution of primordial comets, approximately 100 asteroid families with the parent body size $D_{\rm PB} \geq 100$ km should be created in the main belt during the LHB. Moreover, we expect approximatelyapproximately 10 times more $D_{\rm PB} \geq 100$ km families than $D_{\rm PB} \geq 200$ km. Both facts are in a clear contradiction with observations and we address them in this paper.
*Methods.* We present an updated list of observed asteroid families as identified in the space of synthetic proper elements by the hierarchical clustering method, colour data and dynamical considerations and we estimate their physical parameters. We select 12 families which may be related to the LHB according to their dynamical ages. We then use N-body orbital simulations and collisional models to get insights into long-term dynamical evolution of synthetic LHB families over 4 Gyr. We account for the Yarkovsky/YORP drift in semimajor axis, chaotic diffusion in eccentricity/inclination, possible perturbations by the giant-planet migration, physical disruptions of comets and mutual collisions between family members, comets and main-belt asteroids.
*Results.* The low number of observed LHB families can be explained by the following processes (all of them may actually contribute): i) disruptions of comets below some critical perihelion distance ($q \lesssim 1.5$ AU) are common, ii) asteroid families are destroyed by comminution (via collisional cascade), iii) the size-frequency distribution of the projectiles (comets) was shallow and had an elbow at a larger diameter 100–150 km, iv) physical lifetime of comets was strongly size-dependent so that smaller bodies disrupt easily compared to bigger ones. Our work also serves as a motivation for simulations of high-velocity collisions between hard targets (asteroids) and very weak projectiles (comets) which may result in different outcomes than in low-velocity regimes explored so far.

**Key words.** celestial mechanics – minor planets, asteroids: general – comets: general – methods: numerical

## 1. Introduction

The Late Heavy Bombardment (LHB) is an important period of time in the history of the Solar System, approximately running from 4.1 to 3.8 billion years ago. During this period, most of lunar rocks experienced shock events (Tera et al. 1974) and a large amount of craters and several basins formed on the Moon (Hartmann et al. 2000). It has been suggested that the LHB might have been the tail of an intense bombardment, slowly declining over time since the formation of the Moon and of the terrestrial planets (Neukum et al. 2001, Hartmann et al. 2007, see Chapman et al. 2007 for a review). However, this seems highly implausible on dynamical grounds (Weidenschilling 2000, Bottke et al. 2007). Moreover, if the bombardment history had been as advocated by Neukum et al. (2001), the total amount of mass accreted by the Moon during such declining bombardment would be inconsistent, by one order of magnitude, with the amount of siderophile elements contained in the Lunar crust (Ryder et al., 2000). For these reasons, many scientists, including the authors of this paper, believe that the LHB was a spike in the bombardment history of the Moon and of the inner solar system in general (see for instance Koeberl 2004 or Chapman et al. 2007).

The so-called 'Nice model' provides a coherent explanation of the origin of the LHB as an impact spike. According to this model, the bombardment was triggered by a late dynamical orbital instability of the giant planets, in turn driven by the gravitational interactions between said planets and a massive trans-Neptunian disk of planetesimals (see Morbidelli 2010 for a review). In this model, three projectile populations contributed to the LHB: the comets from the original trans-Neptunian disk (Gomes et al. 2005), the asteroids from the main belt (Morbidelli et al. 2010) and those from a putative extension of the main belt towards Mars, inwards of its current inner edge (Bottke et al. 2011). The latter could have been enough of a source for the LHB, as recorded in the lunar crater record (Bottke et al. 2011), while the asteroids from the current main belt boundaries would have been only a minor contributor (Morbidelli et al. 2010).

The Nice model, however, predicts a very intense cometary bombardment of which there seems to be no trace on the Moon. In fact, given the expected total mass in the original trans-Neptunian disk (Gomes et al. 2005) and the size distribution of objects in said disk (Morbidelli et al. 2009), the Nice model predicts that about $5\times10^4$ km-size comets should have hit the Moon during the LHB. This would have formed 20 km craters with a surface density of $1.7 \times 10^{-3}$ craters per km$^2$. But the highest

crater densities of 20 km craters on the lunar highlands is less than $2 \times 10^{-4}$ (Strom et al. 2005). This discrepancy might be explained by a gross overestimate of the number of small bodies in the original trans-Neptunian disk in Morbidelli et al. (2009). However, all impact clast analyses of samples associated to major LHB basins (Kring and Cohen 2002, Tagle 2005) show that also the major projectiles were not carbonaceous chondrites or similar primitive, comet-like objects.

The lack of evidence for a cometary bombardment of the Moon can be considered as a fatal flaw of the Nice model. Curiously, however, in the outer solar system we see evidence for the cometary flux predicted by the Nice model. Such a flux is consistent with the number of impact basins on Iapetus (Charnoz et al. 2009), with the number and the size distribution of the irregular satellites of the giant planets (Nesvorný et al. 2007, Bottke et al. 2010) and of the Trojans of Jupiter (Morbidelli et al. 2005), as well as with the capture of D-type asteroids into the outer asteroid belt (Levison et al., 2009). Moreover, the Nice model cometary flux is required to explain the origin of the collisional break-up of the asteroid (153) Hilda in the 3/2 resonance with Jupiter (located at $\simeq$ 4 AU, i.e. beyond the nominal outer border of the asteroid belt at $\simeq$ 3.2 AU; Brož et al. 2011).

The lack of an intense cometary bombardment on the Moon and the evidence for a large cometary flux in the outer solar system suggests that the Nice model may be correct in its basic features, but most comets disintegrated as they penetrated deep into the inner solar system.

To support or reject this possibility, this paper focuses at the main asteroid belt, looking for constraints on the flux of comets through this region at the time of the LHB. In particular we focus on old asteroid families, produced by the collisional break-up of large asteroids, which may date back at the LHB time. We provide a census of these families in Section 2, where we also define a "production function" describing the number of families as a function of the size of the respective parent bodies. Interestingly, this function is very shallow, in the sense that there are barely more families with parent bodies of diameter $D_{\rm PB} \simeq 100$ km than those with parent bodies with $D_{\rm PB} = 200$–$400$ km. We also compare the number of young families (estimated age less than 2 Gyr) with that of old families, which reveals a moderate overabundance of old family formation events.

In Section 3, we construct a collisional model of the main belt population. We show that, on average, this population alone could not have produced the observed number of families with $D_{\rm PB} = 200$–$400$ km, even if it was 3 times more populated than now in the past, as advocated in Minton & Malhotra (2010). Also, the production function of families is much steeper than the observed one. However, there is quite a lot of stochasticity in the collisional evolution of the belt, so that some of the realizations of the computer model of said evolution can be consistent with the observations. The likelihood that this happens increases when the assumed specific energy for disruption $Q_D^\star$ of large bodies is decreased.

Instead, the required number of families with large parent bodies is systematically produced if the asteroid belt was crossed by a large number of comets during the LHB, as expected in the Nice model (see Section 4). However, for any reasonable size distribution of the cometary population, the same cometary flux that would produce the correct number of families with $D_{\rm PB} = 200$–$400$ km, would produce too many families with $D_{\rm PB} \simeq 100$ km relative to what is observed. Therefore, in the subsequent sections we look for mechanisms that might prevent detection of most of these families. More specifically, in Sec. 5 we discuss the possibility that families with $D_{\rm PB} \simeq 100$ km are so numerous that they cannot be identified because they overlap with each other. In Sec. 6 we investigate their possible dispersal below detectability due to the Yarkovsky effect and chaotic diffusion. In Sec. 7 we discuss the role of physical lifetime of comets. In Sec. 8 we analyze the dispersal of families due to the changes in the orbits of the giant planets expected in the Nice model. In Sec. 9 we consider the subsequent collisional comminution of the families. Of all investigated processes, the last one seems to be the most promising to reduce the number of visible families with $D_{\rm PB} \simeq 100$ km while not affecting the detectability of old families with $D_{\rm PB} = 200$–$400$ km.

Finally, in Section 10 we analyze a curious portion of the main belt, located in a narrow semi-major axis zone bounded by the 5:2 and 7:3 resonances with Jupiter. This zone is severely deficient in small asteroids compared to the other zones of the main belt. For the reasons explained in the section, we think that this zone best preserves the initial asteroid belt population, and therefore we call it the "pristine zone". We check the number of families in the pristine zone, their sizes and ages and find that they are consistent with the number expected in our model invoking a cometary bombardment at the LHB time and a subsequent collisional comminution and dispersion of the family members.

The conclusions follow in Section 11.

## 2. A list of known families

Although there exist several lists of families in the literature (Zappalá et al. 1995, Nesvorný et al. 2005, Parker et al. 2008, Nesvorný 2010) we are going to identify families once again. The reason is that we seek an *upper limit* for the number of *old families* which may be significantly dispersed and depleted, while the previous works often focused on young and compact clusters. Moreover, we need to calculate several *physical parameters* of the families (like the parent-body size, slopes of the size-frequency distribution, a dynamical age estimate if not available in the literature) which are crucial for further modelling. Last but not least, we use more precise *synthetic* proper elements from the AstDyS database (Knežević & Milani 2003) instead of semi-analytic ones.

We employ a hierarchical clustering method (HCM, Zappalá et al. 1995) for the *initial* identification of families in the proper element space $(a_{\rm p}, e_{\rm p}, \sin I_{\rm p})$, but then we have to perform a lot of manual interaction, because: i) we have to select a reasonable cut-off velocity $v_{\rm cutoff}$, usually such that the dependence of the number of members $N(v_{\rm cutoff})$ is flat. ii) The resulting family should also have a "reasonable" shape in the space of proper elements which shoud somehow correspond to the local dynamical features.[1] iii) We check taxonomic types (colour indices from the Sloan DSS MOC catalogue version 4, Parker et al. 2008) which should be consistent among family members. We can recognise interlopers or overlapping families this way. iv) Finally, the size-frequency distribution should exhibit one or two well-defined slopes, otherwise the cluster is considered uncertain.

Our results are summarised in online Tables 1–3 and the positions of families within the main belt are plotted in Figure 1. Note that our list is "optimistic", so that even not-so-prominent families are included here. If there is no previous estimate for a dynamical age, we can perform either an N-body dynamical modelling, or use a simplified analysis of the proper semimajor axis $a_{\rm p}$ vs absolute magnitude $H$ to get at least an upper limit (as

[1] For example, the Eos family has a complicated but still reasonable shape, since it is determined by several intersecting high-order mean-motion or secular resonances, see Vokrouhlický et al. (2006).

in Vokrouhlický et al. 2006), so that we can distinguish families which are young and old.

There are however several potential problems we are aware of:

1. There may exist *inconsistence* among different lists of families. For example, sometimes a clump may be regarded as a single family or as two separate families. This may be the case of: Lydia and Padua, Rafita and Cameron.
2. We use *synthetic* proper elements for the identification of families which are more precise than the semi-analytic ones. Sometimes the families look more regular (e.g., Teutonia) or more tightly clustered (Beagle) when we use the synthetic elements. This very choice may however affect results substantially! A profound example is the Teutonia family which contains also the *big* asteroid (5) Astraea in the synthetic catalogue but it does *not* in case of the semi-analytic catalogue, because the eccentricity of Astraea is significantly different: $e = 0.2279$ vs 0.1980486. Physical properties of the family then differ vastly, of course.
3. Durda et al. (2007) often claim *larger* size of the parent body (e.g., Themis, Meliboea, Maria, Eos, Gefion, Baptistina), because they try to match the SFD of larger bodies and the results of SPH experiments. This way they account also for small bodies which existed at the time of the disruption, but which do *not* exist today since they were lost due to collisional grinding and the Yarkovsky effect. We prefer to use $D_{\rm Durda}$ if available instead of our value $D_{\rm PB}$ estimated from the currently observed SFD.

### 2.1. A definition of the production function

In order to compare observed families to simulations, we define a "production function" as the cumulative number $N(>D)$ of families with parent-body size $D_{\rm PB}$ larger than given $D$. The observed production function is shown in Figure 2 and it is worth to note that it is very shallow. The number of families with $D_{\rm PB} \simeq 100\,$km is comparable to the number of families in the $D_{\rm PB} = 200$–$400\,$km range.

It is important to note that the observed production function is likely to be affected by biases (the family sample may not be complete, especially below $D_{\rm PB} \lesssim 100\,$km) and also by long-term collisional/dynamical evolution which may prevent a detection of old comminutioned/dispersed families today (Marzari et al. 1999).

From the theoretical point of view, the slope $q$ of the production function $N(>D) \propto D^q$ should correspond to the cumulative slopes of the size-frequency distributions of the target and projectile populations. It is easy to show that the relation is

$$q = 2 + q_{\rm target} + \frac{5}{3} q_{\rm project}\,. \qquad (1)$$

Of course, real populations may have complicated SFDs, with different slopes in different ranges. Nevertheless, any populations which have a steep SFDs (e.g. $q_{\rm target} = q_{\rm project} = -2.5$) would inevitably produce a steep production function ($q \doteq -4.7$).

In the following analysis, we drop cratering events and we discuss catastrophic disruptions only, i.e. families which have largest remnant/parent body ratio smaller than 0.5. The reason is that the same criterion LR/PB < 0.5 is used in collisional models. Moreover, cratering events were not yet systematically explored by SPH simulations due to insufficient resolution (Durda et al. 2007).

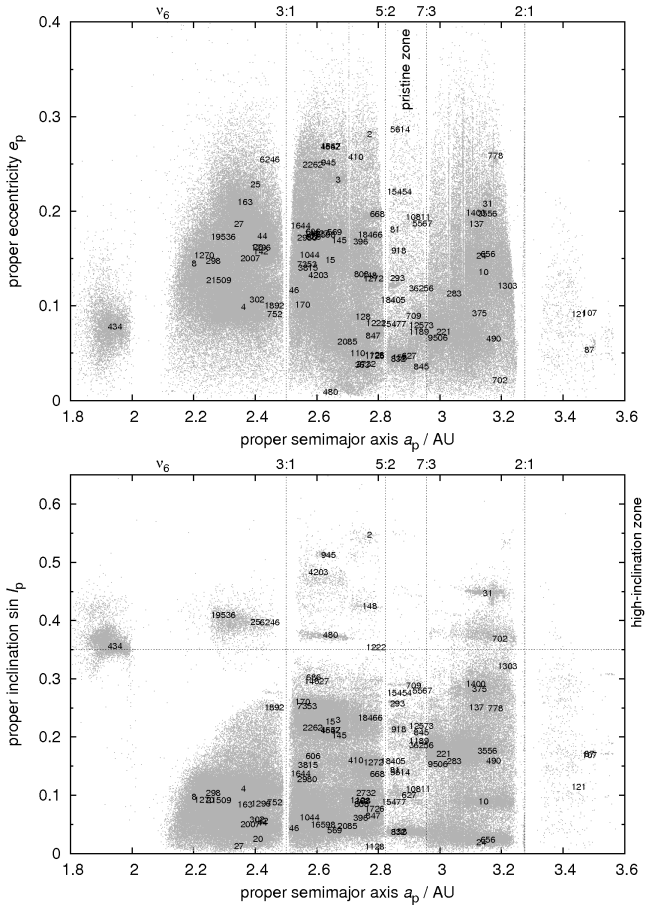


**Fig. 1.** Asteroids from the synthetic AstDyS catalogue plotted in the proper semimajor axis $a_{\rm p}$ vs proper eccentricity $e_{\rm p}$ and $a_{\rm p}$ vs proper inclination sin $I_{\rm p}$ planes. The positions of the identified asteroid families are indicated by the designations of the largest members.

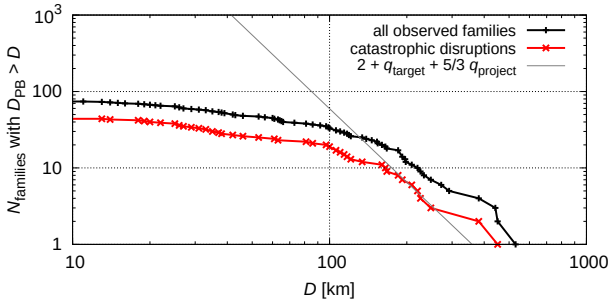


**Fig. 2.** A production function (i.e. the cumulative number $N(>D)$ of families with parent-body size $D_{\rm PB}$ larger than $D$) for all observed families (black) and families corresponding to catastrophic disruptions (red), i.e. with largest remnant/parent body ratio smaller than 0.5. We also plot a theoretical slope according to Eq. 1, assuming $q_{\rm target} = -3.2$ and $q_{\rm project} = -1.2$ which correspond to the slopes of the main belt population in the range $D = 100$–$200\,$km and $D = 15$–$60\,$km, respectively.

### 2.2. Which families can be of LHB origin?

The ages of the observed families and their parent-body sizes are shown in Figure 3. If we compare the number of "young" (<2 Gyr) and old families (>2 Gyr) with $D_{\rm PB} = 200$–$400\,$km we can see a moderate over-abundance of old family formation events. On the other hand, we almost do not observe any small old families.

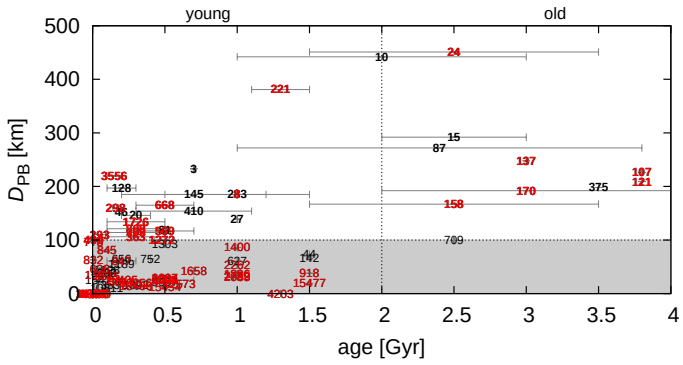


**Fig. 3.** The relation between dynamical ages of families and the sizes of their parent bodies. Every family is denoted by the designation of the largest member. Red labels correspond to catastrophic disruptions while cratering events are labelled black.

**Table 4.** Old families with ages possibly approaching the LHB. They are sorted according to the parent body size, where $D_{\mathrm{Durda}}$ from the Durda et al. (2007) paper is preferred to our estimate $D_{\mathrm{PB}}$. An additional 'c' letter indicates that we extrapolated the SFD slope down to zero $D$, an exclamation mark denotes a significant mismatch with $D_{\mathrm{PB}}$ and $D_{\mathrm{Durda}}$.

| designation | | $D_{\mathrm{PB}}$ (km) | $D_{\mathrm{Durda}}$ (km) | note |
|---|---|---|---|---|
| 24 | Themis | 209c | 451! | |
| 10 | Hygiea | 410 | 442 | cratering |
| 15 | Eunomia | 259 | 292 | cratering |
| 87 | Sylvia | 261 | 272 | cratering |
| 137 | Meliboea | 174c | 248! | |
| 702 | Alauda | 218c | - | high-$I$ |
| 107 | Camilla | >226 | - | non-existent |
| 121 | Hermione | >209 | - | non-existent |
| 375 | Ursula | 198 | - | cratering |
| 170 | Maria | 100c | 192! | |
| 158 | Koronis | 122c | 167 | |
| 709 | Fringilla | 99c | - | cratering |

Only 12 families from the whole list may be *possibly* dated back to the Late Heavy Bombardment, because their dynamical ages approach $\sim 3.8$ Gyr (including their relatively large uncertainties; see Table 4, which is an excerpt from Tables 1–3).

If we drop cratering events and families which do not exist today (their existence was inferred from the satellite systems, Vokrouhlický et al. 2010) we end up with *only* 6 families created by catastrophic disruptions. As we shall see in Section 4, this is an unexpectedly low number.

Moreover, it is really suspicious that most "possibly-LHB" families are larger than $D_{\mathrm{PB}} \simeq 200$ km. It seems that families with $D_{\mathrm{PB}} \simeq 100$ km are missing in the observed sample. This is an important aspect which we have to explain, because it contradics our expectation of a steep production function.

## 3. Collisions in the main belt alone

Before we proceed to scenarios involving the LHB, we try to explain the observed families with ages spanning 0–4 Gyr as a result of collisions only among main-belt bodies. To this purpose, we the collisional code called Boulder (Morbidelli et al. 2009) with the following setup: the intrinsic probabilities $P_{\mathrm{i}} = 3.1 \times 10^{-18}\,\mathrm{km}^{-2}\,\mathrm{yr}^{-1}$, the mutual velocities $V_{\mathrm{imp}} = 5.28$ km/s for the MB vs MB collisions (both were taken from the work of Dahlgren 1998). The scaling law is described by the polynomial relation ($r$ denotes radius in cm):

$$Q_D^\star(r) = \frac{1}{q_{\mathrm{fact}}}\left(Q_0 r^a + B\rho r^b\right) \qquad (2)$$

with the parameters corresponding to basaltic material at 5 km/s (Benz & Asphaug 1999):

| $\rho$ (g/cm$^3$) | $Q_0$ (erg/g) | $a$ | $B$ (erg/g) | $b$ | $q_{\mathrm{fact}}$ |
|---|---|---|---|---|---|
| 3.0 | $7 \times 10^7$ | −0.45 | 2.1 | 1.19 | 1.0 |

We selected the time span of the simulation 4 Gyr (not 4.5 Gyr) since we are interested in this last evolutionary phase of the main belt, when its population and collisional activity is of the same order as today (Bottke et al. 2005). The outcome of a single simulation also depends on the "seed" value of the random-number generator. We thus have to run multiple simulations to obtain information on this stochasticity.

We use the observed SFD of the main belt as the first constraint for our collisional model. However, contrary to Bottke et al. 2005, we do *not* use only a single number to describe the number of observed families (e.g. $N = 20$ for $D_{\mathrm{PB}} \geq 100$ km), but we discuss a complete production function instead. The results in terms of the production function are shown in Figure 4 (left column, 2nd row). On average, the synthetic production function is steeper and *below* the observed one, even though there is approximately a 5 % chance that a single realization of the computer model would resemble the observations quite well. This holds also for the distribution of $D_{\mathrm{PB}} = 200$–$400$ km families in course of the time (age). In the observed sample, there are apparently more old families than young, which may be sometimes produced also in the simulations due to stochasticity.

In this case, the synthetic production function of $D_{\mathrm{PB}} \gtrsim 100$ km families is *not* significantly affected by comminution. According to Bottke et al. (2005), most of $D > 10$ km fragments survive intact and a $D_{\mathrm{PB}} \gtrsim 100$ km family should be recognisable today. This is confirmed also by calculations with Boulder (see Figure 4, left column, 3rd row).

In order to improve the match between the synthetic and observed production function, we can do the following: i) modify the scaling law; ii) account for a dynamical decay of the MB population. Using a substantially lower strength ($q_{\mathrm{fact}} = 5$, which is not likely, thought) one can obtain a synthetic production function which is *on average* consistent with the observations in the $D_{\mathrm{PB}} = 200$–$400$ km range.

Regarding the dynamical decay, Minton & Malhotra (2010) claim that initially the MB was 3 times more populous than today while the decay timescale was very short — after 100 Myr of evolution the number of bodies is almost at the current level. In this brief period of time, about 50 % more families would be created, but all of them would be old, of course. For the remaining $\sim 3.9$ Gyr, the above model (without any dynamical decay) is valid.

To conclude, it is possible – thought not very likely – that the observed families were produced by the collisional activity in the main belt alone. A dynamical decay of the MB population would create more families which are old, but technically speaking, this cannot be distinguished from the LHB scenario, which is to be discussed next.

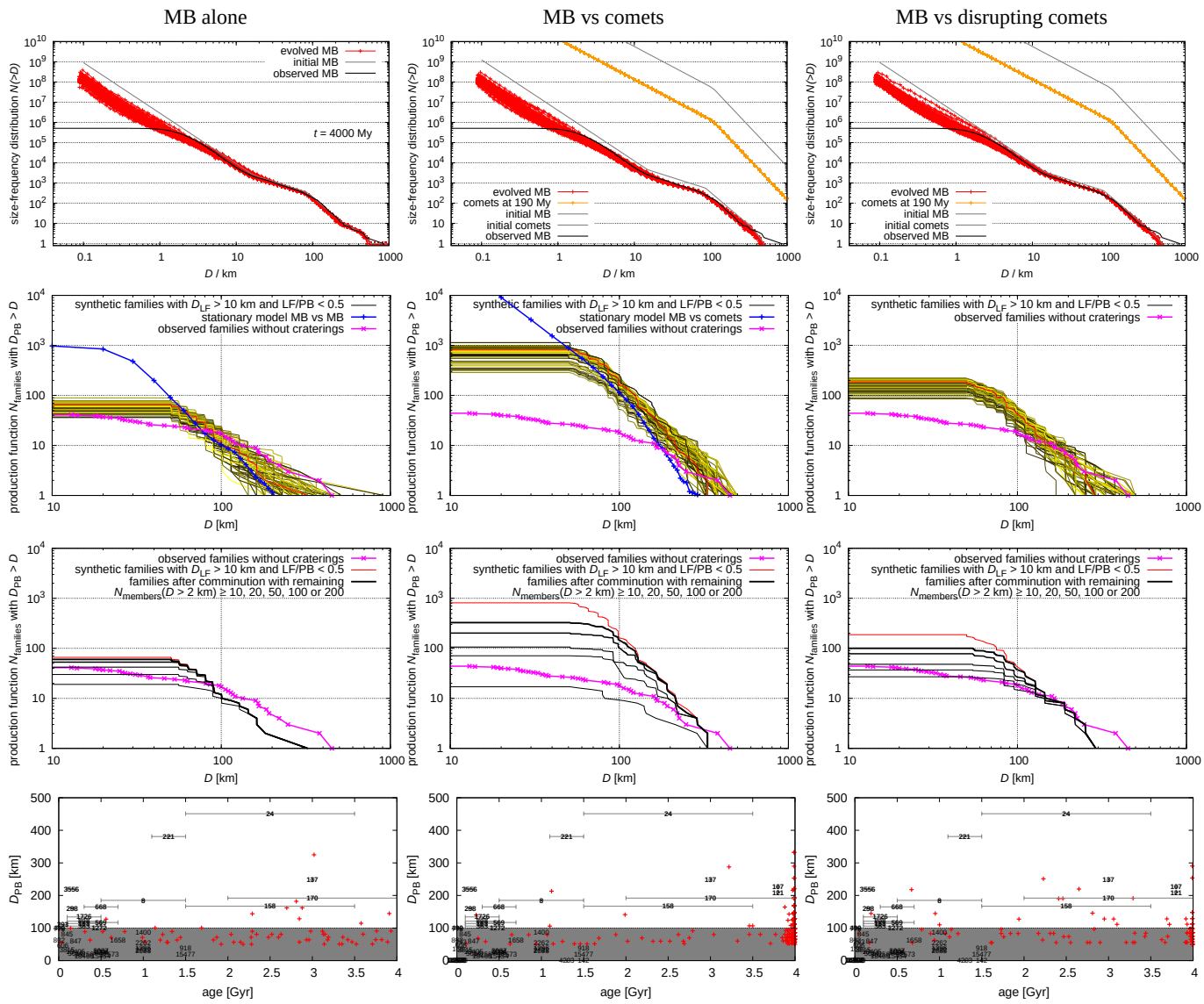


**Fig. 4.** Results of three different collisional models: main-belt alone which is discussed in Section 3 (left column), main-belt and comets from Section 4 (middle column), main-belt and disrupting comets from Section 7 (right column). We always show: the initial and evolved size-frequncy distributions of the populations for 100 Boulder simulations (1st row), the resulting family production function and its comparison to the observations (2nd row), the production function affected by comminution for a selected simulation (3rd row) and the distribution of synthetic families in the (age, $D_{\rm PB}$) plot for a selected simulation (4th row). Note that the positions of synthetic families (red crosses) in the last figure may differ significantly for a different Boulder simulation due to stochasticity and low-number statistics. Moreover, in the middle and right columns, many families were created during the LHB, so there are many overlapping crosses close to 4 Gyr.

## 4. Collisions between a "classical" cometary disk and the main belt

In this section, we are going to construct a collisional model and estimate an expected number of families created during the LHB due to collisions between cometary-disk bodies and main-belt asteroids. We start with a simple stationary model and we confirm the results using a more sophisticated Boulder code (Morbidelli et al. 2009).

Using the data from Vokrouhlický et al. (2008) for a "classical" cometary disk, we can estimate the intrinsic collisional probability and the collisional velocity between comets and asteroids. A typical time-dependent evolution of $P_{\rm i}$ and $V_{\rm imp}$ is shown in Figure 4. The probabilities increase at first, as the transneptunian cometary disk starts to decay, reaching up to $6 \times 10^{-21}\,{\rm km}^{-2}\,{\rm yr}^{-1}$, and after 100 Myr they decrease to zero. These results do *not* differ significantly from run to run.

### 4.1. Simple stationary model

In a stationary collisional model, we choose a SFD for the cometary disk, we assume a *current* population of the main belt, estimate the projectile size necessary to disrupt a given target according to (Bottke et al. 2005)

$$d_{\rm disrupt} = \left(2Q_D^\star / V_{\rm imp}^2\right)^{1/3} D_{\rm target}\,, \tag{3}$$

where $Q_D^\star$ denotes the strength, and finally calculate the number of events during the LHB as

$$n_{\rm events} = \frac{D_{\rm target}^2}{4}\, n_{\rm target} \int P_i(t)\, n_{\rm project}(t)\, {\rm d}t\,. \tag{4}$$

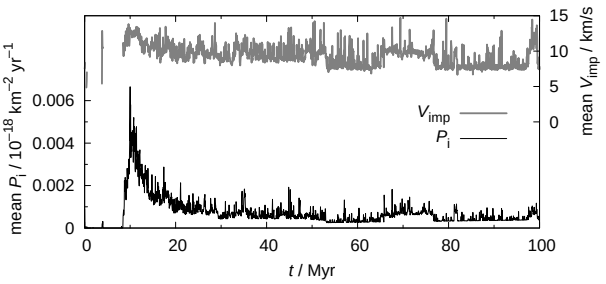


**Fig. 5.** A temporal evolution of the intrinsic collisional probability $P_i$ (bottom) and mean collisional velocity $V_{imp}$ (top) computed for collisions between cometary-disk bodies and the main-belt asteroids.

The actual number of bodies in the simulation (27,000) changes in course of time and it was scaled such that initially it was equal to the number of projectiles $N(>d_{disrupt})$ inferred from the SFD of the disk. This is clearly a *lower limit* for the number of families created, since the main belt was definitely more populous in the past.

The average impact velocity is $V_{imp} \simeq 10\,\mathrm{km/s}$ and we thus need the following projectile sizes to disrupt given target sizes:

| $D_{target}$ (km) | $N_{targets}$ in the MB | $Q^\star_D$ (J/kg) | $d_{disrupt}$ (km) | for $\frac{\rho_{target}}{\rho_{project}} = \frac{3.0}{0.5}$ |
|---|---|---|---|---|
| 100 | ~192 | $1 \times 10^5$ | 12.6 | 23 |
| 200 | ~23 | $4 \times 10^5$ | 40.0 | 73 |

We try to use various SFDs for the cometary disk (i.e., with various differential slopes $q_1$ for $D > D_0$ and $q_2$ for $D < D_0$, the elbow diameter $D_0$ and total mass $M_{disk}$), including rather extreme cases (see Figure 6). The resulting numbers of LHB families are summarised in Table 5. Usually, we obtain several families with $D_{PB} \simeq 200\,\mathrm{km}$ and about 100 families with $D_{PB} \simeq 100\,\mathrm{km}$. This result is robust with respect to the slope $q_2$, because even very shallow SFDs should produce a lot of these families.[2] The only way to decrease the number of families significantly is to assume the elbow at a larger diameter $D_0 \simeq 150\,\mathrm{km}$.

It is thus no problem to explain the existence of approximately 5 *large* families with $D_{PB} = 200$–$400\,\mathrm{km}$ which are indeed observed, since they can be readily produced during the LHB. On the other hand, the high number of $D_{PB} \simeq 100\,\mathrm{km}$ families is clearly contradicting the observations, since we observe *almost no LHB families* of this size. It is also very strange that several $D_{PB} = 200$–$400\,\mathrm{km}$ families exist and $D_{PB} \simeq 100\,\mathrm{km}$ families do *not* exist at the same time! The projectiles capable to disrupt a large parent body are capable to disrupt a small one too, of course.

### 4.2. Constraints from (4) Vesta

The asteroid (4) Vesta presents a significant constraint for collisional models, being a differentiated body with preserved basaltic crust (Keil 2002) and a single large basin on its surface. It is highly unlikely that Vesta experienced a catastrophic disruption in the past and even large cratering events are limited. We thus have to check the number of collisions between one $D = 530\,\mathrm{km}$ target and $D \simeq 35\,\mathrm{km}$ projectiles which are capable to produce the basin and the Vesta family (Thomas et al. 1997). According to Table 5, the number of such events does not exceed ~ 2, so there is a significant chance that Vesta indeed experienced only single impact, given the stochasticity of the results.

[2] The extreme case with $q_2 = 0$ is not likely at all, e.g. because of the continuous SFD of basins on Iapetus and Rhea, which exhibits only a mild depletion of $D \simeq 100\,\mathrm{km}$ size craters; see Kirchoff & Schenk (2010). On the other hand, Sheppard & Trujillo (2010) report an extremely shallow cumulative SFD of Neptune Trojans which is akin to low $q_2$.

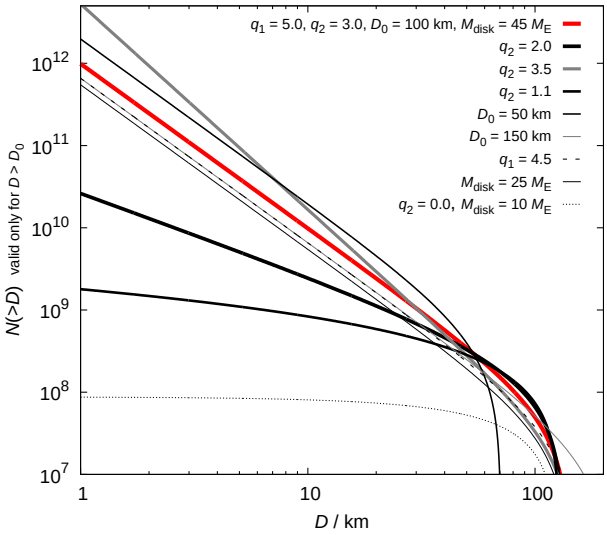


**Fig. 6.** Cumulative size-frequency distributions of the cometary disk which we tested in this work.

### 4.3. Simulations with the Boulder code

In order to confirm results of the simple stationary model, we also perform simulations with the Boulder code. We modified the code to include a time-dependent collisional probabilities $P_i(t)$ and impact velocities $V_{imp}(t)$ of the cometary-disk population.

We start a simulation with a setup resembling the nominal case from Table 5. The scaling law is described by the polynomial relation

$$Q^\star_D(r) = \frac{1}{q_{fact}} \left( Q_0 r^a + B\rho r^b \right) \qquad (5)$$

with the following parameters (the first set corresponds to basaltic material at 5 km/s, Benz & Asphaug 1999):

| | $\rho$ (g/cm$^3$) | $Q_0$ (erg/g) | $a$ | $B$ (erg/g) | $b$ | $q_{fact}$ |
|---|---|---|---|---|---|---|
| asteroids | 3.0 | $7 \times 10^7$ | −0.45 | 2.1 | 1.19 | 1.0 |
| comets | 1.0 | $7 \times 10^7$ | −0.45 | 2.1 | 1.19 | 1.0 |

The intrinsic probabilities $P_i = 3.1 \times 10^{-18}\,\mathrm{km^{-2}\,yr^{-1}}$ and velocities $V_{imp} = 5.28\,\mathrm{km/s}$ for the MB vs MB collisions were again taken from the work of Dahlgren (1998). We do not account for comet–comet collisions since their evolution is dominated by the dynamical decay.

The resulting size-frequency distributions of 100 independent simulations with different random seeds are shown in Figure 4 (middle column). The number of LHB families (approximately 10 with $D_{PB} \simeq 200\,\mathrm{km}$ and 200 with $D_{PB} \simeq 100\,\mathrm{km}$)

**Table 5.** Results of a stationary collisional model between the cometary disk and the main belt. The parameters characterise the SFD of the disk: $q_1$, $q_2$ are differential slopes for the diameters larger/smaller than the elbow diameter $D_0$, $M_{\rm disk}$ denotes the total mass of the disk, and $n_{\rm events}$ is the resulting number of families created during the LHB for a given parent body size $D_{\rm PB}$. The ranges of $n_{\rm events}$ are due to variable density ratios $\rho_{\rm target}/\rho_{\rm project}$ = 1 to 3/1.

| $q_1$ | $q_2$ | $D_0$ (km) | $M_{\rm disk}$ ($M_\oplus$) | $n_{\rm events}$ for $D_{\rm PB} \geq 100$ km | $D_{\rm PB} \geq 200$ km | Vesta craterings | notes |
|---|---|---|---|---|---|---|---|
| 5.0 | 3.0 | 100 | 45 | 115–55 | 4.9–2.1 | 2.0 | nominal case |
| 5.0 | 2.0 | 100 | 45 | 35–23 | 4.0–2.2 | 1.1 | shallow SFD |
| 5.0 | 3.5 | 100 | 45 | 174–70 | 4.3–1.6 | 1.8 | steep SFD |
| 5.0 | 1.1 | 100 | 45 | 14–12 | 3.1–2.1 | 1.1 | extremely shallow SFD |
| 4.5 | 3.0 | 100 | 45 | 77–37 | 3.3–1.5 | 1.3 | lower $q_1$ |
| 5.0 | 3.0 | 50 | 45 | 225–104 | 7.2–1.7 | 3.2 | smaller turn-off |
| 5.0 | 3.0 | 100 | 25 | 64–40 | 2.7–1.5 | 1.1 | lower $M_{\rm disk}$ |
| 5.0 | 3.0 | 100 | 17 | 34 | 1.2 | 1.9 | $\rho_{\rm comets} = 500\,{\rm kg/m^3}$ |
| 5.0 | 3.0 | 150 | 45 | 77–23 | 3.4–0.95 | 0.74 | larger turn-off |
| 5.0 | 0.0 | 100 | 10 | 1.5–1.4 | 0.5–0.4 | 0.16 | worst case (zero $q_2$ and low $M_{\rm disk}$) |

is even *larger* compared to the stationary model, as expected, because we have to start with a larger main belt to get a good fit of the currently observed MB after 4 Gyr of collisional evolution.

To conclude, the stationary model and the Boulder code give compatible results and the mismatch with observed LHB families still holds. We look for a possible explanation in Sections 5–9.

## 5. Can families overlap initially?

Because the number of expected $D_{\rm PB} \geq 100$ km LHB families is very high (of the order 100) we now want to verify if these families can *overlap* in such a way that they cannot be distinguished from each other and from the background. We thus take 192 main-belt bodies with $D \geq 100$ km and select randomly 100 of them which will disrupt. For every one we create an artificial family with $10^2$ members, assume a size-dependent ejection velocity $V \propto 1/D$ (with $V = 50$ m/s for $D = 5$ km) and the size distribution resembling that of the Koronis family. We then calculate proper elements ($a_{\rm p}, e_{\rm p}, \sin I_{\rm p}$) for all bodies.

According to the resulting Figure 7 the answer to the question is simple: the families do *not* overlap sufficiently and they cannot be hidden that way. Moreover, if we take only bigger bodies ($D > 10$ km) these would be clustered even more tightly. The same is true for proper inclinations, which are usually more clustered than eccentricities, so families could be more easily recognised.

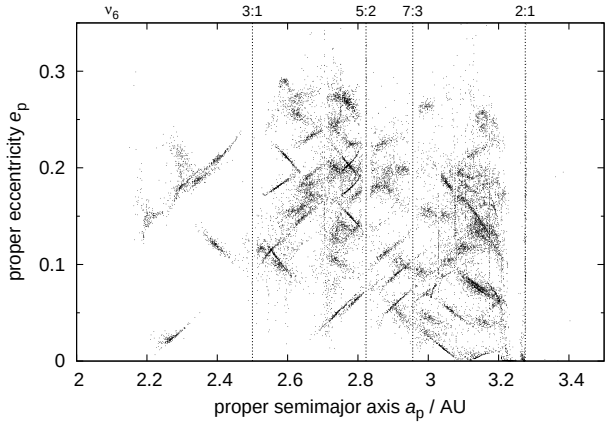


**Fig. 7.** Proper semimajor axis $a_{\rm p}$ vs proper eccentricity $e_{\rm p}$ for 100 synthetic families created in the main belt. It is the *initial* state, shortly after disruption events. We assume the size-frequency distribution of bodies in each synthetic family similar to that of the Koronis family (down to $D \simeq 2$ km).

## 6. Can families be dispersed by the Yarkovsky drift over 4 Gyr?

In this section, we model long-term evolution of synthetic families driven by the Yarkovsky effect and chaotic diffusion. For *one* synthetic family located in the outer belt, we perform a full N-body integration with the SWIFT package (Levison & Duncan 1994), which includes also an implementation of the Yarkovsky/YORP effect (Brož 2006) and 2nd order integrator by Laskar & Robutel (2001). We include 4 giant planets in this simulation. In order to speed-up the integration, we use 10 times smaller sizes of the test particles and thus 10 times shorter time span (400 Myr instead of 4 Gyr). The selected time step is $\Delta t = 91$ d. We compute proper elements, namely their differences $\Delta a_{\rm p}, \Delta e_{\rm p}, \Delta \sin I_{\rm p}$ between the initial and final positions.

Then we use a simple *Monte-Carlo* approach for the whole set of 100 synthetic families — we assign a suitable drift $\Delta a_{\rm p}(D)$ in semimajor axis, and also drifts in eccentricity $\Delta e_{\rm p}$ and inclination $\Delta \sin I_{\rm p}$ to each member of 100 families, respecting asteroid sizes, of course. This way we account for the Yarkovsky semimajor axis drift and also for interactions with mean-motion and secular resonances. Such Monte-Carlo method tends to smear all structures, so we can regard our results as the *upper limits* for dispersion of families.

While the eccentricities of small asteroids (down to $D \simeq 2$ km) seem to be dispersed enough to hide the families, there are still some persistent structures in inclinations (see Figure 8), which would be observable today. Moreover, large asteroids ($D \geq 10$ km) seem to be clustered even after 4 Gyr. We thus can conclude that it is *not* possible to disperse the families by the Yarkovsky effect alone.

## 7. The lifetime of comets in the MB crossing zone

In order to discuss the role of physical lifetime of comets, we had to restart one of the cometary-disk integrations with a fine sampling of the output ($\Delta t_{\rm out} = 500$ yr), because comets usually spend only $10^4$ yr in the main-belt zone (heliocentric distances $\lesssim 3.5$ AU). We then processed the output again and calculated the

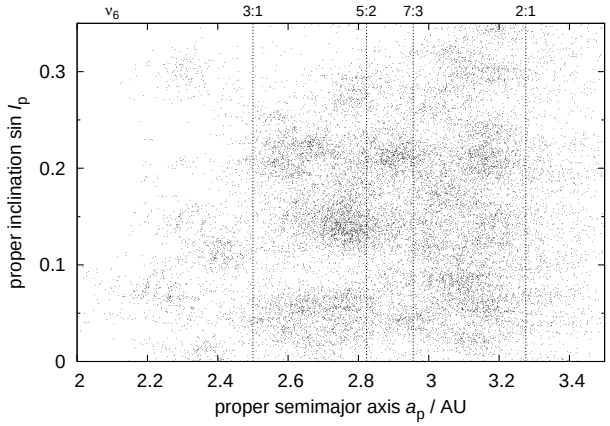


**Fig. 8.** Proper semimajor axis $a_p$ vs proper inclination sin $I_p$ for 100 synthetic asteroid families, *evolved* over 4 Gyr using a Monte-Carlo model. The assumed SFD's correspond to the Koronis family (down to $D \simeq 2$ km).

intrinsic impact probabilities $P_i$ accounting for a simple *comet-disruption criterion*:

$$q < q_{\rm crit} = 1.5\,{\rm AU}\,. \tag{6}$$

This is likely an *upper limit* for disruptions, since the probability of disruption is $p_{\rm crit} = 1$ in this particular case, but it may be lower (and $q$-dependent) in reality.

In case the comets disrupt, the values of $P_i$ are decreased *only by a factor ~3*. Another factor is ~1.5 due to systematically lower mean impact velocities $V_{\rm imp}$ which decrease from 12 km/s to 8 km/s. The resulting number of events is thus decreased by a factor ~4.5 which can be also seen on the production function are summarized in Figure 4 (right column). The production of families with $D_{\rm PB} = 200$–$400$ km is consistent with observations while the number of $D_{\rm PB} \simeq 100$ km families is still too high. Our conclusion is that physical disruptions of comets *cannot* decrease the number of projectiles sufficiently, but the process may partially contribute.

## 8. Perturbation of families by migrating planets (a jumping-Jupiter scenario)

In principle, families created during the LHB may be perturbed by still-migrating planets. It is an open question what was the exact orbital evolution of planets at that time. Nevertheless, a plausible scenario called a "jumping Jupiter" was presented by Morbidelli et al. (2010). It explains major features of the main belt (namely the paucity of high-inclination asteroids above the $\nu_6$ secular resonance), it is consistent with amplitudes of the secular frequencies of both giant and terrestrial planets and also with other features of the Solar System. In this work, we thus investigate this particular migration scenario.

We use the data from Morbidelli et al. (2010) for the orbital evolution of giant planets. We then employ a modified SWIFT integrator, which reads orbital elements for planets from an input file and calculates only the evolution of test particles. Four synthetic families located in the inner/middle/outer belt were integrated. We start the evolution of planets at various times, ranging from $t_0$ to $(t_0 + 4\,{\rm Myr})$ and we stop the integration at $(t_0 + 4\,{\rm My})$, in order to test the perturbation on families created in different phases of migration. Finally, we calculate proper elements of asteroids when the planets do not migrate anymore. (We also have to move planets smoothly to their exact current orbital positions.)

The results are shown in Figure 9. While the proper eccentricities seem to be sufficiently perturbed and families are dispersed even when created at late phases of migration, the proper inclinations pose a problem — they can be only perturbed by the jump itself! This is however in contradiction with the timing of the impactor flux, because most projectiles (comets) reach the main belt *after* the jump, when Neptune is injected to the cometary disk. So most families are created too late to be perturbed.[3]

The conclusion is clear: it is *not* possible to destroy low-$e$ and low-$I$ families by perturbations arising from giant-planet migration, at least in the case of the "jumping-Jupiter" scenario.[4]

## 9. Comminution of asteroid families

We already mentioned that the comminution is *not* sufficient to destroy a $D_{\rm PB} = 100$ km family *in the current environment* of the main belt (Bottke et al. 2005).

However, the situation in case of the LHB scenario is different. Both the large population of comets and several-times larger main belt, which has to withstand the cometary bombardment, contribute to the enhanced comminution of the LHB families. To estimate the amount of comminution, we perform the following calculations: i) for a selected collisional simulation – whose production function is close to the average one – we record the SFD's of all synthetic families created in course of time ii) for each synthetic family, we restart the simulation from the time $t_0$ when the family was crated till 4 Gyr and save the final SFD, i.e. after the comminution. The results are shown in Figure 10.

It is now important to discuss criteria, which enable us to decide if the comminutioned synthetic family would be indeed observable or not. In order to construct the corresponding production function, we use the following set of conditions: $D_{\rm PB} \geq 50$ km, $D_{\rm LF} \geq 10$ km (largest *fragment* is the 1st or the 2nd largest body, where the SFD becomes steep), LR/PB < 0.5 (i.e. a catastrophic disruption). Furthermore, we define $N_{\rm members}$ as the number of the *remaining* family members larger than observational limit $D_{\rm limit} \simeq 2$ km and use a condition $N_{\rm members} \geq 10$. The latter number depends on the position of the family within the main belt, thought. In the favourable "almost-empty" pristine zone $N_{\rm members} \geq 10$ may be valid, but in a populated part of the MB one would need $N_{\rm members} \gtrsim 100$ to detect the family. The size-distributions of synthetic families selected this way resemble the observed SFD's of the main-belt families.

According to Figure 4 (3rd row), where we can see the production functions after comminution for increasing values of $N_{\rm members}$, families with $D_{\rm PB} = 200$–$400$ km remain *more prominent* than $D_{\rm PB} \simeq 100$ km families simply because they contain much more members with $D > 10$ km which survive intact. Our conclusion is thus that comminution may explain the paucity of the observed $D_{\rm PB} \simeq 100$ km families.

[3] Note that high-inclination families would be dispersed much more due to the Kozai mechanism, because eccentricities, which are suffuciently pertrubed, exhibit oscillations coupled with inclinations.

[4] Moreover, the today-non-existent families around (107) Camilla and (121) Hermione — inferred from the existence of their satellites — cannot be destroyed in the jumping-Jupiter scenario, unless the families were actually *pre*-LHB and experienced the jump.

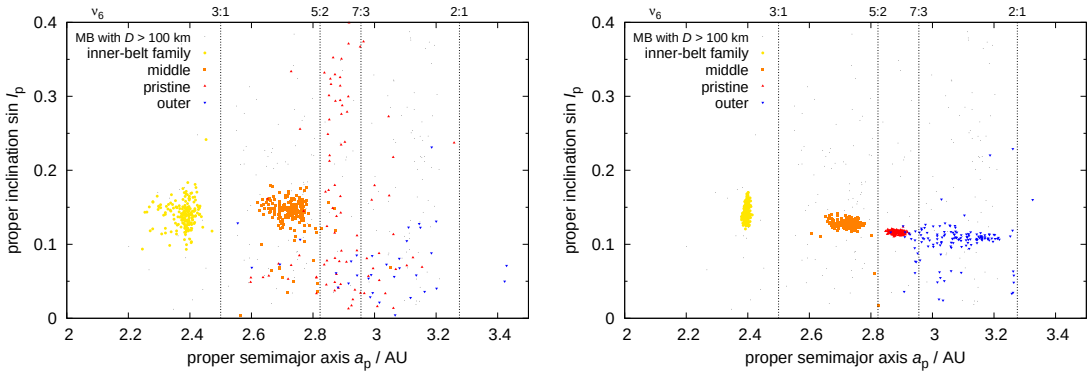


**Fig. 9.** Proper semimajor axis vs proper inclination for four synthetic families (distinguished by symbols) as perturbed by giant-planet migration. Left panel: the simulation spanning the whole interval ($t_0$, $t_0 + 4$ Myr), i.e., including the "jump" due to the encounter between Jupiter and Neptune. Right panel: the simulation beginning just after the jump, i.e. spanning ($t_0 + 1$ Myr, $t_0 + 4$ Myr).

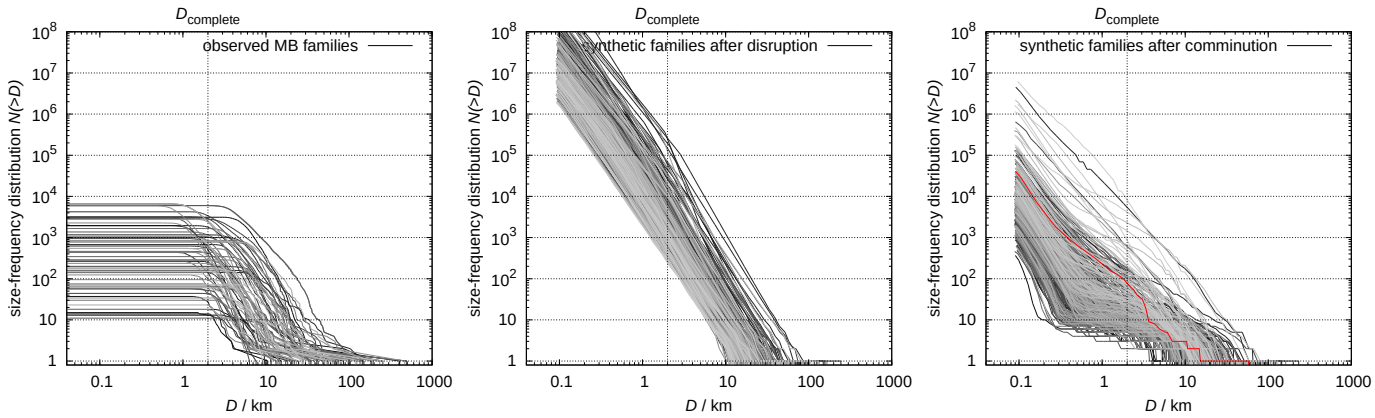


**Fig. 10.** Left panel: the size-frequency distributions of the observed asteroid families. Middle panel: SFD's of 378 distinct synthetic families created during one of the collisional simulations of the MB and comets. Note that initially, all synthetic SFD's are very steep, in agreement with SPH simulations (Durda et al. 2007). We plot only the SFD's which fulfil the following criteria: $D_{\rm PB} \geq 50$ km, $D_{\rm LF} \geq 10$ km, LR/PB $< 0.5$ (i.e. catastrophic disruptions). Right panel: the evolved SFD's after comminution. Only a minority of families is observable now, since the number of remaining members larger that observational limit $D_{\rm limit} \simeq 2$ km is often much smaller than 100. The SFD which we use for the simulation in Section 10 is denoted by red colour.

## 10. "Pristine zone" between the 5:2 and 7:3 resonances

Let us now focus on the zone between the 5:2 and 7:3 resonances, with $a_{\rm p} = 2.825$ to 2.955 AU, which is not so populated as the surrounding regions of the main belt. It thus can be called "pristine zone" because it may resemble the belt *prior* to creation of big asteroid families.

We identified 9 previously unknown small families which are visible on the $(e_{\rm p}, \sin I_{\rm p})$ plot (see Figure 11). They are confirmed by the SDSS colours too. Nevertheless, there is *only one* big family in this zone ($D_{\rm PB} \geq 100$ km), i.e. the Koronis.

The fact that at most one LHB family is observed in the "pristine zone" zone can give us a simple probabilistic estimate for the *maximum* number of disruptions during the LHB. Let us take 192 existing main-belt bodies which have $D \geq 100$ km and select randomly 100 of them which will disrupt. We repeat this selection 1000 times and always count the number of families in the pristine zone. The resulting histogram is shown in Figure 12. As we can see, there is very low (<0.001) probability that the number of families in the pristine zone is zero or one. Mostly, we get 8 families there. It seems that either the number of disruptions should be substantially lower than 100 or we expect to find at least some "remnants" of the LHB families here.

It is interesting that the SFD of an old comminutioned family is *very flat* in the range $D = 1$ to 10 km (see Figure 10) — similarly as some of the "less-certain" observed families! We may speculate that the families like (918) Itha, (5567) Durisen, (12573) 1999 $NJ_{53}$ or (15454) 1998 $YB_3$ (all from the pristine zone) are actually remnants of *larger and older* families, even though they are denoted as younger. May be, the age estimate based on the $(a_{\rm p}, H)$ analysis is incorrect since small bodies were destroyed by comminution and spread by the Yarkovsky effect too far away from the largest remnant, so they can be no more identified with the family.

Finally, we have to ask an important question: how an old/comminutioned family looks like in the proper-element space? To this aim, we created a synthetic family in the "pristine zone", we assumed the family has $N_{\rm members} \simeq 100$ larger than $D_{\rm limit} \simeq 2$ km and the SFD is already flat in the $D = 1$ to 10 km range. We evolved the asteroids up to 4 Gyr due to the Yarkovsky effect and gravitational resonances, using the N-body integrator as in Section 6. Most of the $D \simeq 2$ km bodies were lost in course of the dynamical evolution, of course. The resulting family is shown in Figure 13. We can also imagine that this family is placed in the pristine zone among other observed families, to get a feeling if it is easily observable or not (refer to Figure 11).

It is clear that such family is *hardly observable* even in the almost-empty zone of the main belt! Conclusion is that the com-

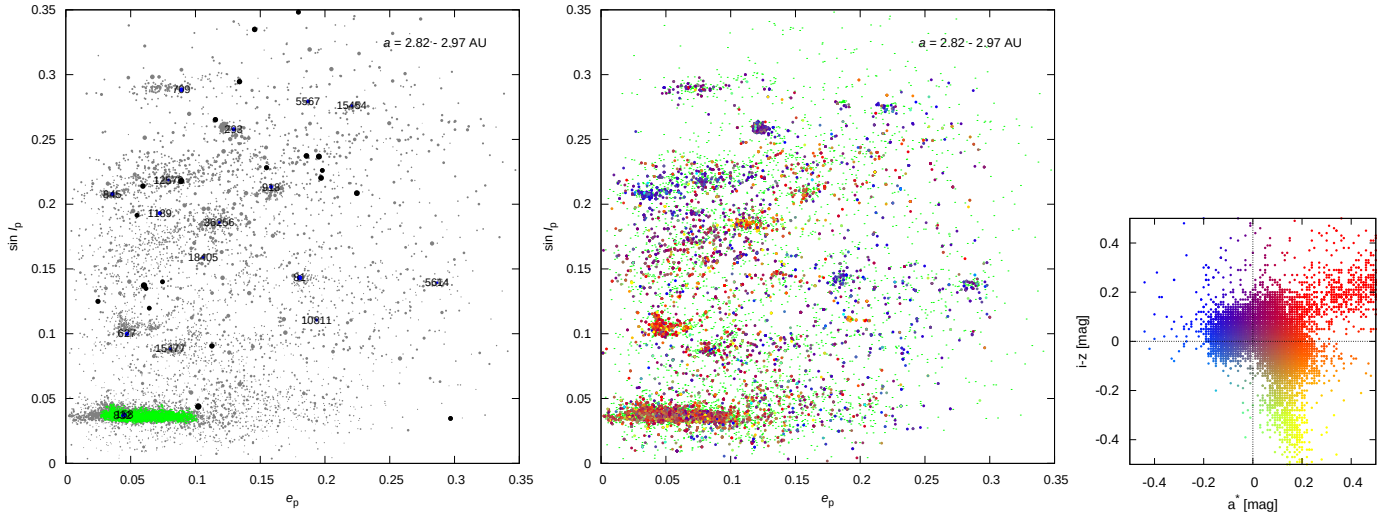


**Fig. 11.** The "pristine zone" of the main belt displayed on the proper eccentricity vs proper inclination plot. Left panel: the sizes of symbols correspond to the sizes of asteroids, red colour is used to emphasize the families. Right panel: colours of symbols correspond to the SDSS colour indices $a^*$ and $i - z$ (Parker et al. 2008).

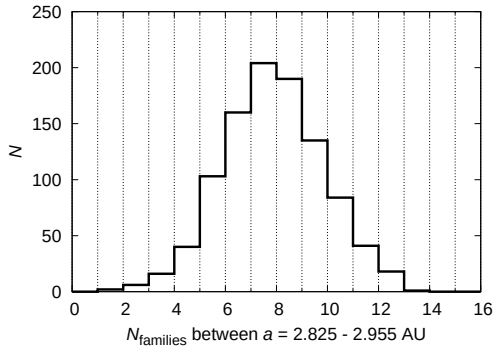


**Fig. 12.** The histogram for the expected number of LHB families located in the "pristine zone" of the main belt.

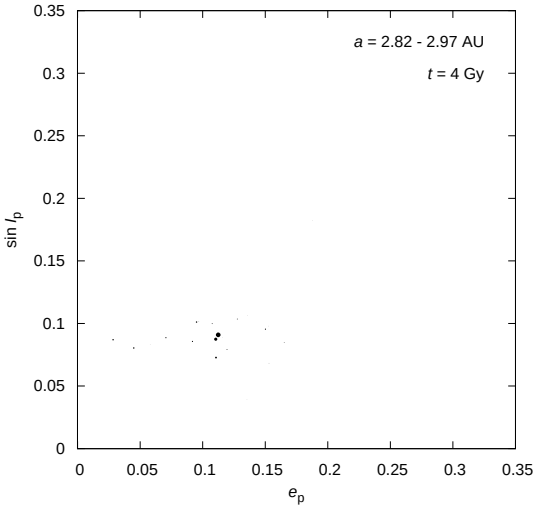


**Fig. 13.** The proper eccentricity vs proper inclination of one synthetic old/comminutioned family evolved dynamically over 4 Gyr. The scales are the same as in Figure 11, se we can compare it easily to the "pristine zone".

minution (as given by the Boulder code) *can explain* the paucity of $D_{\rm PB} \simeq 100$ km LHB families, since we can hardly distinguish old families from the background.

## 11. Conclusions

In this paper, we present two arguments in favour of the Late Heavy Bombardment: i) *on average*, the collisions in the main belt alone do not produce enough catastrophic disruptions to explain the existence of $D_{\rm PB} = 200$–$400$ km families; ii) the number of these families does not seem to be uniformly distributed in time, although this may be a result of stochasticity in the collisional evolution.

On the other hand, if we assume a nominal cometary flux across the main belt – as predicted by the Nice model – the big families with $D_{\rm PB} = 200$–$400$ km are produced systematically. We can obtain even better agreement with observations in case the flux was about 1/5 of the nominal one, which would correspond to a situation when comets frequently disrupt in the vicinity of the Sun.

We also address the apparent contradiction between the high expected number of LHB families with parent-body size $D_{\rm PB} \geq 100$ km (about 100) and the low observed number (at most 12). Moreover, we expect many more $D_{\rm PB} \geq 100$ km families than $D_{\rm PB} \geq 200$ km which is in contradiction with observations too.

The following possibilities seem to be ruled-out:

1. Even a shallow SFD of *projectiles* (comets) with the elbow diameter 50 to 100 km is capable to produce a lot of families.
2. Families cannot be simply "hidden" due to an overlapping in the $(a_{\rm p}, e_{\rm p}, \sin I_{\rm p})$ space.
3. The Yarkovsky drift $\mathrm{d}a/\mathrm{d}t$ and chaotic diffusion in $e/I$ due to resonances do *not* disperse families sufficiently in the inclination space.
4. The giant-planet migration (in a jumping-Jupiter scenario) again does *not* perturb inclinations enough.

We are thus left with five explanations (all of them may actually contribute):

1. Frequent disruptions of comets below $q < 1.5$ AU can decrease the number of families down to $\sim 30$.
2. The comminution can destroy $D_{\rm PB} \simeq 100$ km families almost completely, while the "cores" of $D_{\rm PB} = 200$ km families remain more prominent.
3. The SFD of the *projectiles* (comets) had the elbow at a larger diameter 100–150 km, and the total number of comets

was much smaller than $10^9$ in the relevant size range $D$ = 10 to 70 km. Such SFD may be also in concert with the cratering record of the Moon, but if comets disrupt often below $q < 1.5$ AU then the cratering does not constrain their SFD at all. On the other hand, we may need up to $10^{12}$ small of comets ($D \simeq 1$ km) to create the Oort cloud which favours steep SFD's.

4. Physical lifetime of comets may be strongly size-dependent, so $D$ = 10 to 20 km comets (which serve as projectiles for $D_{\rm PB} \simeq 100$ km bodies) disrupt easily compared to $D$ = 40 to 70 km comets (producing $D_{\rm PB} \simeq 200$ km families).
5. Collisions between *hard targets* (i.e. rocky asteroids) and *extremely weak projectiles* (active icy comets) at high impact velocities $V_{\rm imp} \simeq 12$ km/s may have a different physics. Note that comets sometimes disintegrate from internal/outgassing reasons (i.e. *without* any collision). The energy consumed by phase transitions during impact may play an important role too. This is a different regime which have not been explored before by SPH simulations (P. Michel, personal communication) and our work thus may serve as a motivation for further studies.

To conclude, we have no definitive answer to the question what was the size-frequency distribution of the cometary disk and the flux of comets across the main belt, but we identified five important processes which may explain why we do *not* observe many families from the LHB time, even though collisional models predict they were indeed created.

Further observations of small Neptune Trojans, which are believed to be an intact ancient population, may provide independent constraints of the cometary-disk SFD. We would also need more information on physical lifetimes of *new* (Oort cloud) comets which are poorly known today because of small statistics.

## Acknowledgements

The work of MB and DV has been supported by the Grant Agency of the Czech Republic (grants 205/08/P196 and 205/08/0064) and the Research Program MSM0021620860 of the Czech Ministry of Education. We also acknowledge the usage of computers of the Observatory and Planetarium in Hradec Králové.

## References

Benz, W., Asphaug, E., 1999, Icarus, 142, 5
Bottke, W.F., Vokrouhlický, D., Brož, M., Nesvorný, D., Morbidelli, A., 2001, Science, 294, 1693
Bottke, W.F., Durda, D.D., Nesvorný, D., Jedicke, R., Morbidelli, A., Vokrouhlický, D., Levison, H.F., 2005, Icarus, 175, 111
Bottke, W.F., Levison, H.F., Nesvorný, D., Dones, L., 2007, Icarus, 190, 203
Bottke, W.F., Vokrouhlický, D., Nesvorný, D., 2007, Nature, 449, 48
Bottke, W.F., Vokrouhlický, D., Nesvorný, D., Minton, D., Morbidelli, A., Brasser, R., 2010, LPI Conf., 41, 1269
Bottke, W.F., Nesvorný, D., Vokrouhlický, D., Morbidelli, A., 2010, AJ, 139, 994
Brož, M., 2006, PhD thesis, Charles Univ.
Brož, M., Vokrouhlický, D., Morbidelli, A., Nesvorný. D., Bottke, W.F., 2011, MNRAS, 414, 2716
Carruba, V., 2009, MNRAS, 398, 1512
Carruba, V., 2010, MNRAS, 408, 580
Chapman, C.R., Cohen, B.A., Grinspoon, D.H., 2007, Icarus, 189, 233
Charnoz, S., Morbidelli, A., Dones, L., Salmon, J., 2009, Icarus, 199, 413
Cohen, B.A., Swindle, T.D., Kring, D.A., 2000, Science, 290, 1754
Dahlgren, M., 1998, A&A, 336, 1056
Durda, D.D., Bottke, W.F., Nesvorný, D., Enke, B.L., Merline, W.J., Asphaug, E., Richardson, D.C., 2007, 186, 498
Foglia, S., Masi, G., 2004, Minor Planet Bull., 31, 100
Gil-Hutton, R., 2006, Icarus, 183, 83
Gomes, R., Levison, H.F., Tsiganis, K., Morbidelli, A., 2005, Nature, 435, 466
Hartmann, W.K., Quantin, C., Mangold, N., 2007, Icarus, 186, 11
Hartmann, W.K., Ryder, G., Dones, L., Grinspoon, D., 2000, in Origin of the Earth and Moon, ed. R.M. Canup, K. Righter, Tucson: University of Arizona Press, p. 493
Keil, K., 2002, in Asteroids III, ed. W.F. Bottke Jr., A. Cellino, P. Paolicchi, R.P. Binzel, Tucson: University of Arizona Press, p. 573
Kirchoff, M.R., Schenk, P., 2010, Icarus, 206, 485
Knežević, Z., Milani, A., 2003, A&A, 403, 1165
Koeberl, C., 2004, Geochimica et Cosmochimica Acta, 68, 931
Kring, D.A., Cohen, B.A., 2002, J. Geophys. Res., 107, 41
Laskar, J., Robutel, P., 2001, Celest. Mech. Dyn. Astron., 80, 39
Levison, H.F., Duncan, M., 1994, Icarus, 108, 18
Levison, H.F., Bottke, W.F., Gounelle, M., Morbidelli, A., Nesvorný, D., Tsiganis, K., 2009, Nature, 460, 364
Margot, J.-L., Rojo, P., 2007, BAAS, 39, 1608
Marzari, F., Farinella, P., Davis, D.R., 1999, Icarus, 142, 63
Michel, P., Tanga, P., Benz, W., Richardson, D.C., 2002, Icarus, 160, 10
Michel, P., Jutzi, M., Richardson, D.C., Benz, W., 2011, Icarus, 211, 535
Minton, D.A., Malhotra, R., 2010, Icarus, 207, 744
Morbidelli, A., Tsiganis, K., Crida, A., Levison, H.F., Gomes, R., 2007, AJ, 134, 1790
Morbidelli, A., 2010, Comptes Rendus Physique, 11, 651
Morbidelli, A., Brasser, R., Gomes, R., Levison, H.F., Tsiganis, K., 2010, AJ, 140, 1391
Morbidelli, A., Levison, H.F., Bottke, W.F., Dones, L., Nesvorný, D., 2009, Icarus, 202, 310
Molnar, L.A., Haegert, M.J., 2009, BAAS, 41, 2705
Nesvorný, D., Morbidelli, A., Vokrouhlický, D., Bottke, W.F., Brož, M., 2002, Icarus, 157, 155
Nesvorný, D., Jedicke, R., Whiteley, R.J., Ivezić, Ž., 2005, Icarus, 173, 132
Nesvorný, D., Vokrouhlický, D., 2006, AJ, 132, 1950
Nesvorný, D., Vokrouhlický, D., Morbidelli, A., 2007, AJ, 133, 1962
Nesvorný, D., Vokrouhlický, D., Morbidelli, A., Bottke, W.F., 2009, Icarus, 200, 698
Nesvorný, D., 2010, EAR-A-VARGBDET-5-NESVORNYFAM-V1.0, NASA Planetary Data System
Neukum, G., Ivanov, B.A., Hartmann, W.K., 2001, Space Sci. Rev., 96, 55
Novaković, B., 2010, MNRAS, 407, 1477
Novaković, B., Tsiganis, K., Knežević, Z., 2010, Celest. Mech. Dyn. Astron., 107, 35
Novaković, B., Cellino, A., Knežević, Z., 2011, Icarus, in press
Parker, A., Ivezić, Ž., Jurić, M, Lupton, R., Sekora, M.D., Kowalski, A., 2008, Icarus, 198, 138
Ryder, G., Koeberl, C., Mojzsis, S.J., 2000, in Origin of the Earth and Moon, ed. R.M. Canup, K. Righter, Tucson: University of Arizona Press, p. 475
Sheppard, S.S, Trujillo, C.A., 2010, ApJL, 723, L233
Strom, R.G., Malhotra, R., Ito, T., Yoshida, F., Kring, D.A., 2005, Science, 309, 1847.
Tagle, R., 2005, LPI Conf., 36, 2008
Tedesco, E.F., Noah, P.V., Noah, M., Price, S.D., 2002, AJ, 123, 1056
Tera, F., Papanastassiou, D.A., Wasserburg, G.J., 1974, Earth & Planet. Sci. Let., 22, 1
Thomas, P.C., Binzel, R.P., Gaffey, M.J., Storrs, A.D., Wells, E.N., Zellner, B.H., 1997, Science, 277, 1492
Vokrouhlický, D., Brož, M., Bottke, W.F., Nesvorný, D., Morbidelli, A., 2006, Icarus, 182, 118
Vokrouhlický, D., Nesvorný, D., Levison, H.F., 2008, AJ, 136, 1463
Vokrouhlický, D., Nesvorný, D., Bottke, W.F., Morbidelli, A., 2010, AJ, 139, 2148
Vokrouhlický, D., Nesvorný, D., 2011, AJ, 142, 26
Warner, B.D., Harris, A.W., Vokrouhlický, D., Nesvorný, D., Bottke, W.F., 2009, Icarus, 204, 172
Weidenschilling, S.J., 2000, Space Sci. Rev., 92, 295
Zappalà, V., Bendjoya, Ph., Cellino, A., Farinella, P., Froeschlé, C., 1995, Icarus, 116, 291

**Table 1.** A list of asteroid families and their physical parameters. There are the following columns: $v_{\rm cutoff}$ is the selected cut–off velocity for the hierarchical clustering, $N$ the corresponding number of family members, $p_V$ the adopted value of the geometric albedo (from Tedesco et al. 2002, if unknown the 0.15 value is used for the calculation of $D_{\rm PB}$), taxonomic classification (according to the Sloan DSS MOC 4 colours, Parker et al. 2008), $D_{\rm PB}$ parent body size, an additional 'c' letter indicates that we prolonged the SFD slope down to zero $D$ (a typical uncertainty is 10 %), $D_{\rm Durda}$ PB size from SPH simulations (Durda et al. 2007), an exclamation mark denotes a significant mismatch with $D_{\rm PB}$, LR/PB the ratio of the volumes of the largest remnant to the parent body (an uncertainty corresponds to the last figure, a range is given if both $D_{\rm PB}$ and $D_{\rm Durda}$ are known), $v_{\rm esc}$ the escape velocity, $q_1$ the slope of the SFD for larger $D$, $q_2$ the slope for smaller $D$ (a typical uncertainty of the slopes is 0.1, if not indicated otherwise), dynamical age including its uncertainty. In case there is a reference in the last column is followed by '…', it is valid until a next empty line.

| designation | | $v_{\rm cutoff}$ m/s | $N$ | $p_V$ | tax. | $D_{\rm PB}$ km | $D_{\rm Durda}$ km | LR/PB | $v_{\rm esc}$ m/s | $q_1$ | $q_2$ | age Gyr | notes, references |
|---|---|---|---|---|---|---|---|---|---|---|---|---|---|
| 3 | Juno | 50 | 449 | 0.250 | S | 233 | ? | 0.999 | 139 | −4.9 | −3.2 | <0.7 | cratering, Nesvorný et al. (2005) … |
| 4 | Vesta | 110 | 12672 | 0.434 | V | 530 | 425! | 0.996 | 313 | −4.0 | −2.9 | <3.0 | old? but steep SFD, cratering |
| 8 | Flora | 60 | 6554 | 0.250 | S/C | 141 | 185 | 0.878-0.39 | 84 | −2.4 | −2.8 | 1.0 ± 0.5 | cut by $\nu_6$ resonance, LL chondrites |
| 10 | Hygiea | 70 | 3122 | 0.055 | C,B | 410 | 442 | 0.976-0.78 | 243 | −4.2 | −3.2 | 2.0 ± 1.0 | LHB? cratering |
| 15 | Eunomia | 50 | 2867 | 0.187 | S | 259 | 292 | 0.958-0.66 | 153 | −5.6 | −2.3 | 2.5 ± 0.5 | LHB? Michel et al. (2002) |
| 20 | Massalia | 40 | 2980 | 0.215 | S | 146 | 144 | 0.995 | 86 | −5.0 | −3.0 | 0.3 ± 0.1 | |
| 24 | Themis | 50 | 2100 | 0.126 | C | 209c | 451! | 0.123-0.012 | 120 | −3.9 | −2.1 | 2.5 ± 1.0 | LHB? |
| 44 | Nysa (Polana) | 70 | 6165 | 0.562 | S | >73 | ? | 0.88 | 44 | −8.0 | −2.6(0.5) | <1.5 | overlaps with (142) Polana |
| 46 | Hestia | 65 | 95 | 0.053 | S | 124 | 153 | 0.992-0.53 | 74 | −3.3 | −2.0 | <0.2 | cratering, close to J3/1 resonance |
| 87 | Sylvia | 110 | 71 | 0.045 | C/X | 261 | 272 | 0.994-0.88 | 154 | −5.2 | −2.4 | 1.0-3.8 | LHB? cratering, Vokrouhlický et al. (2010) |
| 128 | Nemesis | 60 | 654 | 0.052 | C | 189 | 197 | 0.987-0.87 | 112 | −3.4 | −3.3 | 0.2 ± 0.1 | |
| 137 | Meliboea | 95 | 199 | 0.054 | C | 174c | 248! | 0.59-0.20 | 102 | −1.9 | −1.8 | <3.0 | old? |
| 142 | Polana (Nysa) | 60 | 154 | 0.046 | C | >66 | ? | 0.60 | 38 | ? | −4.1 | <1.5 | overlaps with (44) Nysa |
| 145 | Adeona | 50 | 1161 | 0.065 | C | 171c | 185 | 0.688-0.54 | 101 | −5.2 | −2.8 | 0.7 ± 0.5 | cut by J5/2 resonance |
| 158 | Koronis | 50 | 4225 | 0.147 | S | 122c | 167 | 0.024-0.009 | 68 | −3.6(0.3) | −2.3 | 2.5 ± 1.0 | LHB? |
| 163 | Erigone | 60 | 1059 | 0.056 | C/X | 79 | 114 | 0.787-0.26 | 46 | ? | −3.6 | 0.3 ± 0.2 | |
| 170 | Maria | 80 | 3209 | 0.220 | S | 100c | 192! | 0.086-0.012 | 59 | −2.7 | −2.6 | 3.0 ± 1.0 | LHB? |
| 221 | Eos | 50 | 5976 | 0.130 | K | 208c | 381! | 0.125-0.020 | 123 | −3.5 | −2.1 | 1.3 ± 0.2 | |
| 283 | Emma | 75 | 345 | 0.050 | - | 152 | 185 | 0.916-0.508 | 90 | ? | −3.2 | <1.0 | satellite |
| 293 | Brasilia | 60 | 282 | 0.055? | C/X | 57 | 110 | 0.127-0.018 | 34 | −1.6 | −3.4 | 0.05 ± 0.04 | (293) is interloper |
| 363 | Padua (Lydia) | 80 | 287 | 0.087 | C/X | 76 | 106 | 0.045-0.017 | 45 | −1.8 | −3.2 | 0.3 ± 0.2 | |
| 396 | Aeolia | 20 | 124 | 0.171 | C/X | 35 | 39 | 0.966-0.70 | 20 | ? | −4.3 | <0.1 | cratering |
| 410 | Chloris | 90 | 259 | 0.057 | C | 126c | 154 | 0.952-0.52 | 74 | ? | −2.1 | 0.7 ± 0.4 | |
| 490 | Veritas | - | - | - | C,P,D | - | 100-177 | - | - | - | - | 0.0083 ± 0.0005 | (490) is likely interloper (Michel et al. 2011) |
| 569 | Misa | 70 | 543 | 0.031 | C | 88c | 117 | 0.578-0.25 | 52 | −3.9 | −2.3 | 0.5 ± 0.2 | |
| 606 | Brangane | 30 | 81 | 0.102 | S | 37 | 46 | 0.918-0.48 | 22 | ? | −3.8 | 0.05 ± 0.04 | |
| 668 | Dora | 50 | 837 | 0.054 | C | 85 | 165! | 0.031-0.004 | 50 | −4.2 | −1.9 | 0.5 ± 0.2 | |
| 808 | Merxia | 50 | 549 | 0.227 | S | 37 | 121! | 0.66-0.018 | 22 | −2.7 | −3.4 | 0.3 ± 0.2 | |
| 832 | Karin | - | - | - | S | - | 63 | - | - | - | - | 0.0058 ± 0.0002 | |
| 845 | Naema | 30 | 173 | 0.081 | C | 77c | 81 | 0.353-0.30 | 46 | −5.2 | −2.9 | 0.1 ± 0.05 | |
| 847 | Agnia | 40 | 1077 | 0.177 | S | 39 | 61 | 0.38-0.10 | 23 | −2.8 | −3.1 | 0.2 ± 0.1 | |
| 1128 | Astrid | 50 | 265 | 0.079 | C | 43c | ? | 0.522 | 25 | −1.7 | −2.6 | 0.1 ± 0.05 | |
| 1272 | Gefion | 60 | 19477 | 0.20 | S | 74c | 100-150! | 0.001-0.004 | 60 | −4.3 | −2.5 | 0.48 ± 0.05 | Nesvorný et al. (2009), L chondrites |
| 1400 | Tirela | 80 | 1001 | 0.070 | S | 86 | - | 0.12 | 86 | −4.2 | −3.4 | <1.0 | |
| 1644 | Rafita | 70 | 621 | 0.15? | S | 42c | 63 | 0.07 | 25 | −3.8 | −2.5 | 1.5 ± 0.5 | |
| 1726 | Hoffmeister | 40 | 822 | 0.035 | C | 93c | 134 | 0.022-0.007 | 55 | −4.5 | −2.7 | 0.3 ± 0.2 | |
| 3556 | Lixiaohua | 60 | 439 | 0.055? | C/X | 60 | 220! | 0.029-0.001 | 35 | −5.0 | −3.5 | 0.15 ± 0.05 | Novaković et al. (2010) |
| 3815 | Konig | 60 | 177 | 0.044 | C | 33 | ? | 0.32 | 20 | ? | −3.0 | <0.1 | (1639) Bower is interloper |
| 4652 | Iannini | - | - | - | S | - | - | - | - | - | - | 0.005 ± 0.005 | |
| 9506 | Telramund | 40 | 1466 | 0.15? | S | 25 | - | 0.05 | 15 | −7.5 | −2.7 | <0.5 | |
| 18405 | 1993 $FY_{12}$ | 50 | 44 | 0.055? | C/X | 26 | - | 0.23 | 15 | ? | −2.8 | <0.2 | cut by J5/2 resonance |

**Table 2.** A continuation of Table 1.

| designation | | $v_{cutoff}$ m/s | $N$ | $p_V$ | tax. | $D_{PB}$ km | $D_{Durda}$ km | LR/PB | $v_{esc}$ m/s | $q_1$ | $q_2$ | age Gyr | notes, references |
|---|---|---|---|---|---|---|---|---|---|---|---|---|---|
| 158 | Koronis$_{(2)}$ | - | - | - | S | 35 | - | - | - | - | - | 0.015 ± 0.005 | cratering, Molnar & Haegert (2009) |
| 298 | Baptistina | 50 | 1661 | 0.035 | C/X | 90c | 160! | 0.133 | 48 | −5.9 | −2.3 | 0.16 ± 0.02 | buried in (8) Flora, Bottke et al. (2007), K/T event |
| 434 | Hungaria | 200 | 4598 | 0.35 | E | 25 | - | 0.148 | 15 | −5.9 | −3.1 | 0.5 ± 0.2 | Warner et al. (2010) |
| 627 | Charis | 80 | 235 | 0.081 | S | >60 | - | 0.53 | 35 | ? | −3.4 | <1.0 | |
| 778 | Theobalda | 85 | 154 | 0.060 | C | 97c | - | 0.29 | 57 | ? | −2.9 | 0.007 ± 0.002 | cratering, Novaković (2010) |
| 302 | Clarissa | 30 | 75 | 0.054 | C | 39 | - | 0.961 | 23 | ? | −3.1 | <0.1 | cratering, Nesvorný (2010) … |
| 656 | Beagle | 24 | 63 | 0.089 | C | 64 | - | 0.562 | 38 | −1.3 | −1.4 | <0.2 | |
| 752 | Sulamitis | 60 | 191 | 0.042 | C | 65 | - | 0.833 | 39 | −6.5 | −2.3 | <0.4 | |
| 1189 | Terentia | 50 | 18 | 0.070 | C | 56 | - | 0.990 | 33 | ? | −2.6? | <0.2 | cratering |
| 1892 | Lucienne | 100 | 57 | 0.15? | S | 15 | - | 0.643 | 9 | ? | −3.8 | <0.3 | |
| 7353 | Kazvia | 50 | 23 | 0.15? | S | 16 | - | 0.645 | 9 | ? | −1.7 | <0.1 | |
| 10811 | Lau | 100 | 15 | 0.15? | S | 11 | - | 0.796 | 7 | ? | −2.7? | <0.1 | |
| 18466 | 1995 SU$_{37}$ | 40 | 71 | 0.15? | S | 14 | - | 0.032 | 9 | ? | −4.8 | <0.3 | |
| 1270 | Datura | - | - | - | S | - | - | - | - | - | - | 0.00045-0.00060 | identified in osculating-element space, |
| 14627 | Emilkowalski | - | - | - | C/X | - | - | - | - | - | - | 0.00019-0.00025 | Nesvorný & Vokrouhlický (2006) … |
| 16598 | 1992 YC$_2$ | - | - | - | S | - | - | - | - | - | - | 0.00005-0.00025 | |
| 21509 | Lucascavin | - | - | - | S | - | - | - | - | - | - | 0.0003-0.0008 | |
| 2384 | Schulhof | - | - | - | S | - | - | - | - | - | - | 0.0007-0.0009 | Vokrouhlický & Nesvorný (2011) |
| 27 | Euterpe | 70 | 268 | 0.15? | S | 139 | - | 0.998 | 82 | −2.8 | −2.0 | <1.0 | cratering, Parker et al. (2008) … |
| 110 | Lydia (Padua) | - | - | - | - | - | - | - | - | - | - | <0.06 | merges with (363) Padua |
| 375 | Ursula | 80 | 777 | 0.057 | C | 198 | - | 0.762 | 117 | −4.1 | −2.3 | <3.5 | old? |
| 1044 | Teutonia | 50 | 1950 | 0.343 | S | 27-120 | - | 0.17-0.98 | 16-71 | −3.5 | −3.9 | <0.5 | depends on (5) Astraea membership |
| 1296 | Andree | 60 | 439 | 0.15? | S | 37-68 | - | 0.04-0.94 | 22-40 | ? | −2.5 | <1.0 | depends on (79) Eurynome membership |
| 2007 | McCuskey | 34 | 236 | 0.06 | C | 29 | - | 0.411 | 17 | ? | −5.6 | <0.5 | overlaps with (44) Nysa/Polana |
| 2085 | Henan | 54 | 946 | 0.15? | S | 31 | - | 0.206 | 18 | −4.2 | −2.8 | <1.0 | |
| 2262 | Mitidika | 83 | 462 | 0.055? | C | 53 | - | 0.046 | 31 | −3.6 | −2.4 | <1.0 | (785) Zwetana is interloper?, overlaps with (3) Juno |
| 2 | Pallas | 200 | 64 | 0.163 | B | 498c | - | 0.9996 | 295 | ? | −2.2 | <0.5 | high-$I$, Carruba (2010) … |
| 25 | Phocaea | 160 | 1370 | 0.22 | S | 92 | - | 0.540 | 55 | −3.1 | −2.4 | <2.2 | old? high-$I/e$, cut by $\nu_6$ resonance, Carruba (2009) |
| 148 | Gallia | 150 | 57 | 0.169 | S | 98 | - | 0.058 | 58 | ? | −3.6 | <0.45 | high-$I$ |
| 480 | Hansa | 150 | 651 | 0.256 | S | 60 | - | 0.825 | 35 | −4.9 | −3.2 | <1.6 | high-$I$ |
| 686 | Gersuind | 130 | 178 | 0.146 | S | 52c | - | 0.482 | 40 | ? | −2.7 | <0.8 | high-$I$, Gil-Hutton (2006) |
| 945 | Barcelona | 110 | 129 | 0.248 | S | 28 | - | 0.771 | 16 | ? | −3.5 | <0.35 | high-$I$, Foglia & Masi (2004) |
| 1222 | Tina | 110 | 37 | 0.338 | S | 21 | - | 0.936 | 12 | ? | −4.1 | <0.15 | high-$I$ |
| 4203 | Brucato | - | - | - | - | - | - | - | - | - | - | <1.3 | in freq. space |
| 31 | Euphrosyne | 100 | 851 | 0.056 | C | 259 | - | 0.968 | 153 | −4.9 | −3.9 | <1.5 | cratering, high-$I$, Foglia & Massi (2004) |
| 702 | Alauda | 120 | 791 | 0.070 | B | 218c | - | 0.025 | 129 | −3.9 | −2.4 | <3.5 | old? high-$I$, cut by J2/1 resonance, satellite (Margot & Rojo 2007) |
| 107 | Camilla | ? | ? | 0.054 | - | >226 | ? | ? | ? | ? | ? | 3.8? | LHB? Cybele region, non-existent today, |
| 121 | Hermione | ? | ? | 0.058 | - | >209 | ? | ? | ? | ? | ? | 3.8? | LHB? Vokrouhlický et al. (2010) … |

**Table 3.** A continuation of Table 1.

| designation | | $v_{\rm cutoff}$ m/s | $N$ | $p_V$ | tax. | $D_{\rm PB}$ km | $D_{\rm Durda}$ km | LR/PB | $v_{\rm esc}$ m/s | $q_1$ | $q_2$ | age Gyr | notes, references |
|---|---|---|---|---|---|---|---|---|---|---|---|---|---|
| 1303 | Luthera | 100 | 142 | 0.043 | X | 92 | - | 0.808 | 54 | −3.9 | −2.7 | <0.5 | above (375) Ursula, new suggested families … |
| 1547 | Nele | 20 | 57 | 0.15? | X | 26 | - | 0.851 | 15 | ? | −2.5 | <0.04 | close to (3) Juno |
| 2732 | Witt | 60 | 985 | 0.15? | S | 33 | - | 0.062 | 20 | −4.1 | −3.8 | <1.0 | only part with $\sin I > 0.099$, above (363) Padua |
| 81 | Terpsichore | 120 | 70 | 0.052 | C | 119 | - | 0.993 | 71 | ? | −4.4 | <0.5 | cratering, less-certain new families in the "pristine zone" … |
| 709 | Fringilla | 140 | 60 | 0.047 | X | 99c | - | 0.931 | 59 | −6.2 | −1.7 | <2.5 | old? |
| 918 | Itha | 140 | 63 | 0.23 | S | 38 | - | 0.157 | 22 | −2.7 | −1.5 | <1.5 | strange SFD |
| 5567 | Durisen | 100 | 18 | 0.15? | X | 21 | - | 0.845 | 13 | ? | −2.0 | <0.5 | strange SFD |
| 5614 | Yakovlev | 100 | 34 | 0.05 | C | 22 | - | 0.278 | 13 | ? | −3.2 | <0.2 | |
| 12573 | 1999 $NJ_{53}$ | 40 | 13 | 0.15? | C | 18 | - | 0.120 | 10 | ? | −1.9 | <0.6 | incomplete SFD |
| 15454 | 1998 $YB_3$ | 50 | 14 | 0.15? | C | 13 | - | 0.374 | 8 | ? | −1.4 | <0.5 | strange SFD |
| 15477 | 1999 $CG_1$ | 110 | 144 | 0.15? | S | 19 | - | 0.067 | 11 | ? | −5.1 | <1.5 | |
| 36256 | 1999 $XT_{17}$ | 60 | 30 | 0.15? | S | 20 | - | 0.068 | 12 | ? | −1.4 | <0.3 | strange SFD |